MEASUREMENT OF CHROMATIC RESONANCE DRIVING TERMS IN THE LHC

M. Stefanelli*[1], E. Maclean, European Organization for Nuclear Research, Geneva, Switzerland
[1]also at National Institute for Subatomic Physics, Amsterdam, Netherlands

Abstract

The $3Q_y$ resonance is of particular concern at LHC injection given its potential to degrade the lifetime and the machine dynamic aperture. During measurements of the chromatic linear optics for the 2025 LHC commissioning, a large variation of the $3Q_y$ resonance strength across different momentum deviations δ was observed. Further studies were performed to assess the contribution to this variation from higher order multipoles, in particular from octupole and decapole fields. Benchmarking has been performed to the LHC magnetic model revealing that skew-octupole (a_4) errors in the main dipoles alone cannot explain the observed skew-octupole field sources at injection. Methods and results of this analysis are presented in this report.

INTRODUCTION

Resonances $(j-k)Q_x + (l-m)Q_y$ are characterized by the strength of their respective resonance driving terms (RDT), f_{jklm}. Of particular interest for LHC is the $3Q_y$ resonance that has been shown to degrade beam lifetime at 450 GeV [1] and to contribute to collimator hierarchy breakage [2]. For these reasons, this resonance was closely monitored during LHC commissioning in 2025. Of particular note was the large variation in the $3Q_y$ resonance amplitude across different momentum deviations δ. On-momentum, the $3Q_y$ resonance is driven by skew-sextupolar magnetic fields. Correction schemes have been implemented in the LHC to correct the on-momentum $3Q_y$ resonance at injection energy [3]. However, when a particle is off-momentum in a dispersive region, effective skew-sextupole components can be generated through feed-down from higher-order fields. This study focuses on characterizing the impact of skew-octupole and skew-decapole magnetic fields, present in the machine as magnetic imperfections. The Hamiltonians for skew-octupole and skew-decapole magnets follow,

$$S_4(x,y) = -\frac{1}{24}J_4\left(4x^3y - 4xy^3\right), \tag{1a}$$

$$S_5(x,y) = -\frac{1}{120}J_5\left(5x^4y - 10x^2y^3 + y^5\right), \tag{1b}$$

where J_n is the normalized strength of the skew multipole of order n. If a particle has a relative momentum deviation $\delta \neq 0$, its transverse position is shifted in dispersive regions according to $x \rightarrow x + D_x\delta$. Substituting this into the Hamiltonians above introduces new terms proportional to powers of δ. Of particular interest are those terms that feed-down to an effective skew-sextupole term, as these directly drive the $3Q_y$ resonance. The skew-octupole expanded Hamiltonian is given by

$$S_4(x,y,\delta) = -\frac{1}{24}J_4\left(4x^3y - 4xy^3\right) - \frac{D_x\delta J_4}{6}\left(3x^2y - y^3\right) - \frac{D_x^2\delta^2 J_4}{2}(xy) + \frac{D_x^3\delta^3 J_4}{6}(-y), \tag{2}$$

where the arising skew-sextupole terms $\left(3x^2y - y^3\right)$, multiplied by $D_x\delta$, can be identified directly. In the case of the skew-decapole feed-down, the same terms appear multiplied by $D_x^2\delta^2$ instead. It follows directly that a linear dependence of the skew-sextupole Hamiltonian on δ indicates feed-down from skew-octupole components J_4, while a quadratic dependence indicates feed-down from skew-decapole components J_5. Note that Eq. (2) accounts only for the pure skew-octupole contribution; other sources, such as normal-octupole fields in the presence of coupling, and feed-up from lower-order fields with or without coupling, also contribute to the total effective skew-octupole field. Analyzing the momentum dependence of the $3Q_y$ RDT therefore serves two purposes: it directly characterizes how the resonance strength varies with momentum, and it provides an indirect means of probing higher-order multipole fields that cannot otherwise be directly measured.

MEASUREMENTS

The results presented here were obtained during LHC Run 3 commissioning in 2025. The original goal of the shift was to fully commission the injection optics at 450 GeV. The chromaticity was corrected to approximately 3 units in each plane with the main sextupole magnets (MS). The RF frequency was varied by scanning values from −350 Hz to 350 Hz in steps of 50 Hz. This corresponds to a relative momentum deviation δ ranging between ±0.0025. Turn-by-Turn (TbT) data were acquired via forced oscillations induced with an AC dipole [4, 5]. The machine tune feedback system (QFB) [6] was kept on during the entire measurement time to ensure a constant natural tune and AC dipole frequency offset [7], avoiding bias in the forced RDT measurement due to moving closer to or further from the resonance, as δ was varied [8]. The QFB varies the tuning quadrupoles (MQT) powering, keeping the tunes constant while minimally perturbing the optics. The nominal on-momentum tunes for the injection optics are $Q_x = 62.28$ and $Q_y = 60.31$. With the corrected chromaticity $Q' = 3.0$, the maximum tune shift being compensated is approximately ±0.0075, a small fraction of the nominal tune. The AC dipole frequency offsets in tune units were equal to $\Delta Q_x = -0.010$ and $\Delta Q_y = 0.012$. Typically, large AC

* mattia.stefanelli@cern.ch

dipole excitations are needed to perform clear and reliable RDT measurements. For the considered measurements, the induced excitation remains coherent over the 6600 turns of the acquisition window, ensuring high-quality spectral analysis. An example of AC dipole excitation is shown in Fig. 1, where we can observe the stable driven oscillation lasting for the entire turn window. A zero-padded FFT (HARPY) [9], with a noise reduction via SVD cleaning, was subsequently applied to the acquired data to retrieve the frequency spectrum. For AC dipole forced oscillations, the f_{0030} RDT drives the vertical spectral line at ACD $-2Q_y$ [8, 10]. The spectral analysis results are shown in Fig. 2 for a sample BPM in LHC Beam 1 (B1), BPM.10L4.B1, for some of the tested momentum deviations. Since the AC dipole perturbs the particle motion, the resulting frequency spectrum is also modified; the measured RDTs are therefore forced quantities that differ from the free RDTs [8, 11].

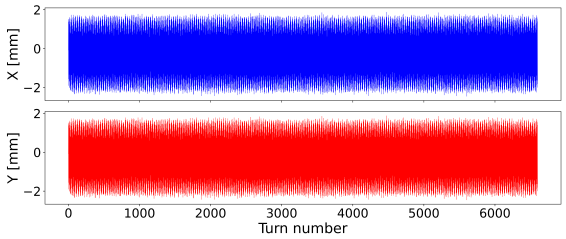

Figure 1: AC dipole excitation in both transverse planes.

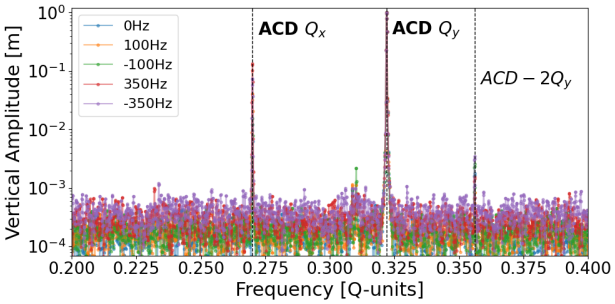

Figure 2: Vertical frequency spectra over multiple acquisitions with different δ values.

The action of the QFB is clearly visible from the tunes remaining constant in the spectrum. This is crucial for an optimal RDT measurement, as any tune variation would distort the measured resonance amplitude, preventing the isolation of the pure momentum dependence. Optics parameters are calculated from the acquired spectrum to retrieve the amplitude, real, and imaginary components of the different RDTs. The f_{0030} amplitude, for a selection of tested δ values, is presented in Fig. 3 for both LHC B1 and B2. Outliers present in the Insertion Regions (IRs) have been removed. The amplitude variation observed off-momentum is much larger than the on-momentum value, suggesting that for off-momentum particles at injection energy, the dominant contribution comes from higher-order multipole fields rather than from skew-sextupole fields themselves.

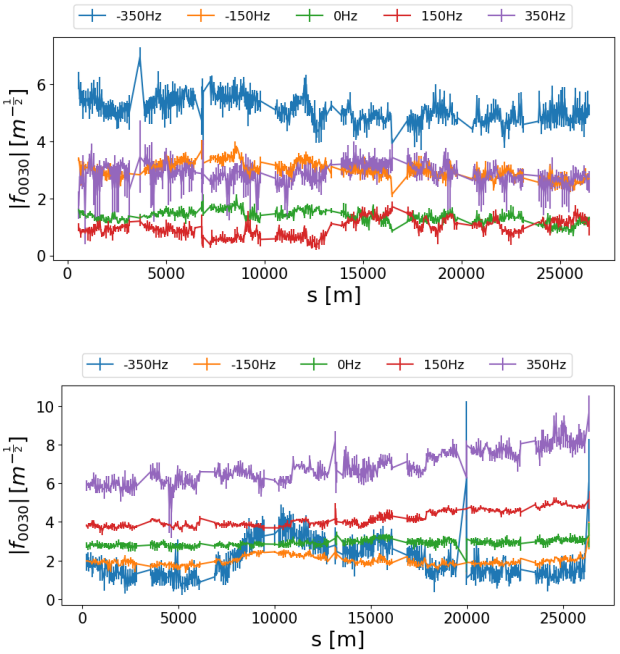

Figure 3: f_{0030} amplitude, across different momentum deviations, for LHC B1 (top) and B2 (bottom).

ANALYSIS

To characterize the momentum dependence of the forced f_{0030}, the real and imaginary parts were analyzed separately across all tested momentum deviations. Both can be expressed as a Taylor expansion around the on-momentum value, carried out to second order to capture contributions from both feed-down sources under investigation: the first-order coefficient describes the linear momentum dependence driven by skew-octupole fields, while the second-order coefficient captures the quadratic dependence arising from skew-decapole fields. At each BPM, the real and imaginary parts of f_{0030} were measured across all tested momentum deviations, as described in the previous section, and fitted with a second-order polynomial function.

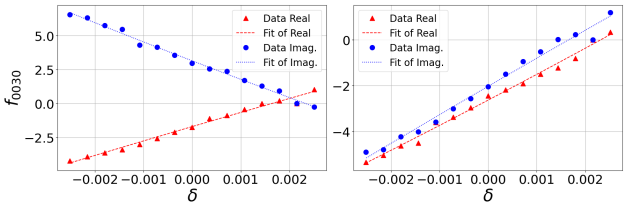

Figure 4: Measurement and fit for 2 example BPMs.

Results for two example BPMs in arcs 23 and 34 are shown in Fig. 4. The first-order coefficients for the full ring are presented in blue in Fig. 5, while the second-order coefficients are shown in blue in Fig. 6. Results are shown for B1, with analogous results obtained for B2. Insets showing a zoom of arc 34 are included for clarity.

Consistent results are observed across all arcs. To quantify the relative importance of each term, the first- and second-order contributions of the Taylor expansion are evaluated

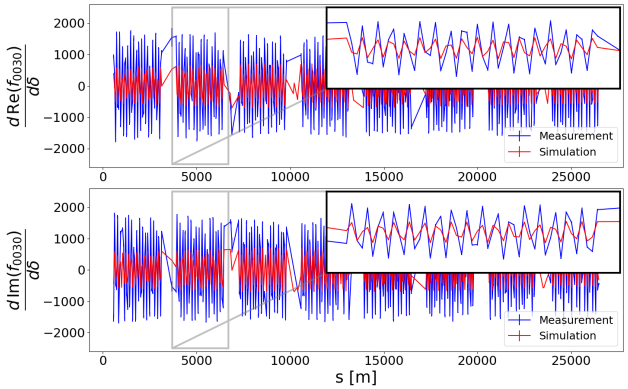

Figure 5: Linear momentum dependence coefficients for the f_{0030} RDT.

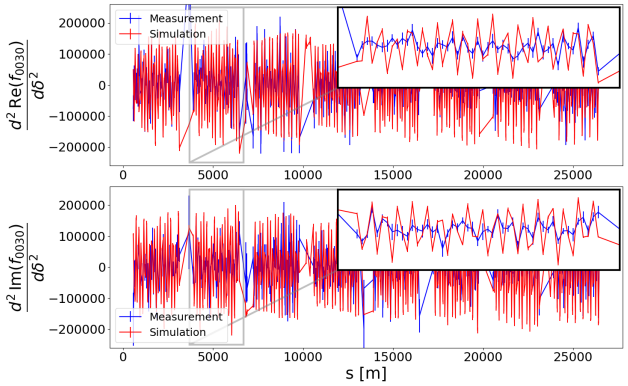

Figure 6: Second-order momentum dependence coefficients for the f_{0030} RDT.

directly at a test momentum deviation of $\delta = 0.0025$. The results are shown in Fig. 7. For the real component, the average of the second-order contribution taken along the ring is a factor of 10.02 smaller than the linear term; for the imaginary part, the corresponding ratio is 20.89. Consistent results were observed for B2. These results indicate that, within the tested range of δ and for the LHC at injection energy with the 2025 optics configuration, the momentum dependence of the $3Q_y$ resonance is predominantly linear, and thus primarily driven by skew-octupole fields.

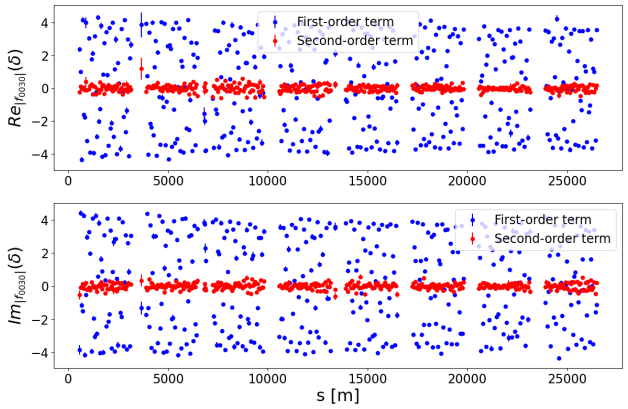

Figure 7: Comparison of the first and second-order terms.

Model Benchmarking

As a second step, the results are benchmarked against the LHC model. A best-knowledge model with injection optics was used to study the chromatic behavior of the $3Q_y$ resonance. Random and systematic skew-octupole (a_4) errors in the main dipoles were introduced according to the Field Description for the LHC (FiDeL) [12]. AC dipoles were included in the simulations, and particles were tracked for 10000 turns across several momentum deviations δ. The effect of the QFB was accounted for by matching the tunes to their nominal on-momentum values, consistent with what was done during the measurements. The same analysis procedure applied to the measurements was then applied to the simulated TbT data to extract the momentum-dependent coefficients. Simulation results are shown in red in Figs. 5 and 6 for LHC B1. While the simulations correctly reproduce the phase of the RDT, the magnitude of the linear momentum-dependence coefficients is underestimated by approximately a factor of 2 for both the real and imaginary parts, as visible in the insets. The second-order dependence, despite its smaller magnitude, is reasonably well reproduced by the model. This discrepancy suggests that a_4 errors in the dipoles are a major source of skew-octupole fields but that alone they cannot reproduce the measurement, pointing to the need to expand the model to also include other sources.

CONCLUSIONS

The chromatic behavior of the $3Q_y$ resonance has been studied to evaluate skew-octupole and skew-decapole contributions in the LHC. The RDT exhibits a predominantly linear momentum dependence, consistent with feed-down from skew-octupole fields, while the second-order term, indicative of skew-decapole sources, is shown to be small in comparison. Benchmarking against the current LHC model reveals that the FiDeL a_4 errors in the main dipoles alone are insufficient to account for the observed skew-octupole fields, pointing to the presence of additional sources to be identified and benchmarked.

ACKNOWLEDGMENTS

Thanks to the LHC OP and OMC teams for their support.

REFERENCES

[1] E. Maclean *et al.*, "3Qy resonance correction at LHC injection", in *Proc. IPAC'25*, Taipei, Taiwan, pp. 1964–1967, Nov. 2025. doi:10.18429/JACoW-IPAC2025-WEPM008

[2] R. Tomas *et al.*, "Mitigation of losses at injection protection devices in the CERN LHC", in *Proc. IPAC'23*, Venice, Italy, pp. 547–550, Sep. 2023. doi:10.18429/JACoW-IPAC2023-MOPL019

[3] E. Waagaard and E. H. Maclean, "A Response Matrix Approach to Skew-Sextupole Correction in the LHC at Injection", in *Proc. IPAC'22*, Bangkok, Thailand, pp. 1987–1990, Jul. 2022. doi:10.18429/JACoW-IPAC2022-WEPOPT058

[4] R. Tomás, "Adiabaticity of the ramping process of an ac dipole", *Phys. Rev. ST Accel. Beams*, vol. 8, no. 2, p. 024401, Feb. 2005. doi:10.1103/PhysRevSTAB.8.024401

[5] E. Carlier, L. Ducimetière, and E. B. Vossenberg, "A Kicker Pulse Generator for Measurement of the Tune and Dynamic Aperture in the LHC", *Conference Record of the 2006 Twenty-Seventh International Power Modulator Symposium*, pp. 463–466, 2006. https://api.semanticscholar.org/CorpusID:25269610

[6] L. Grech, G. Valentino, D. Alves, and S. Hirlaender, "Application of reinforcement learning in the LHC tune feedback", *Front. Phys.*, vol. 10, p. 929064, 2022. doi:10.3389/fphy.2022.929064

[7] J. Serrano and M. Cattin, "The LHC AC dipole system: an introduction", *CERN-BE-Note-2010-014 (CO)*, 2010. https://cds.cern.ch/record/1263248

[8] R. Tomás, "Normal form of particle motion under the influence of an ac dipole", *Phys. Rev. ST Accel. Beams*, vol. 5, no. 5, p. 054001, May 2002. doi:10.1103/PhysRevSTAB.5.054001

[9] L. Malina, "Harpy: A Fast, Simple and Accurate Harmonic Analysis with Error Propagation", in *Proc. IPAC'22*, Bangkok, Thailand, pp. 2326–2329, Jul. 2022. doi:10.18429/JACoW-IPAC2022-WEPOMS035

[10] A. Franchi, R. Tomás, and F. Schmidt, "Magnet strength measurement in circular accelerators from beam position monitor data", *Phys. Rev. ST Accel. Beams*, vol. 10, no. 7, p. 074001, Jul. 2007. doi:10.1103/PhysRevSTAB.10.074001

[11] A. Wegscheider and R. Tomás, "Forced Coupling Resonance Driving Terms", in *Proc. IPAC'21*, Campinas, Brazil, May 2021, pp. 3646–3649. doi:10.18429/JACoW-IPAC2021-WEPAB400

[12] L. Bottura *et al.*, "First Field Test of FiDeL the Magnetic Field Description for the LHC", in *Proc. PAC'09*, Vancouver, Canada, May 2009, paper MO6PFP046, pp. 241–243. https://jacow.org/PAC2009/papers/MO6PFP046.pdf